

Deterministic modeling of the diffusive memristor

Cite as: Chaos **31**, 073111 (2021); <https://doi.org/10.1063/5.0056239>

Submitted: 07 May 2021 • Accepted: 21 June 2021 • Published Online: 07 July 2021

 A. Akther,  Y. Ushakov,  A. G. Balanov, et al.

COLLECTIONS

Paper published as part of the special topic on [In Memory of Vadim S. Anishchenko: Statistical Physics and Nonlinear Dynamics of Complex Systems](#)



View Online



Export Citation



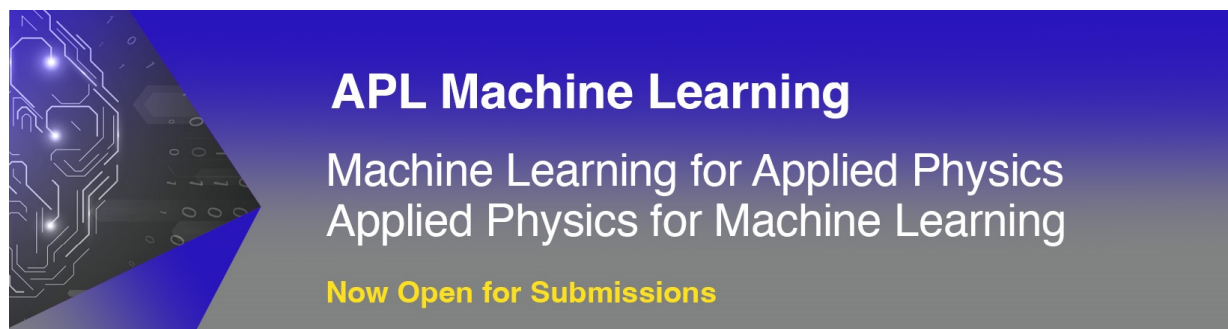
CrossMark

ARTICLES YOU MAY BE INTERESTED IN

[Brain-inspired computing with memristors: Challenges in devices, circuits, and systems](#)
Applied Physics Reviews **7**, 011308 (2020); <https://doi.org/10.1063/1.5124027>

[A comprehensive review on emerging artificial neuromorphic devices](#)
Applied Physics Reviews **7**, 011312 (2020); <https://doi.org/10.1063/1.5118217>

[Reliability of analog resistive switching memory for neuromorphic computing](#)
Applied Physics Reviews **7**, 011301 (2020); <https://doi.org/10.1063/1.5124915>



APL Machine Learning
Machine Learning for Applied Physics
Applied Physics for Machine Learning
Now Open for Submissions

Deterministic modeling of the diffusive memristor

Cite as: Chaos 31, 073111 (2021); doi: 10.1063/5.0056239

Submitted: 7 May 2021 · Accepted: 21 June 2021 ·

Published Online: 7 July 2021



View Online



Export Citation



CrossMark

A. Akther,^{a)} Y. Ushakov, A. G. Balanov, and S. E. Savel'ev

AFFILIATIONS

Department of Physics, Loughborough University, Loughborough LE11 3TU, United Kingdom

Note: This paper is part of the Focus Issue, In Memory of Vadim S. Anishchenko: Statistical Physics and Nonlinear Dynamics of Complex Systems.

^{a)} Author to whom correspondence should be addressed: A.Akther@lboro.ac.uk

ABSTRACT

Recently developed diffusive memristors have gathered a large amount of research attention due to their unique property to exhibit a variety of spiking regimes reminiscent to that found in biological cells, which creates a great potential for their application in neuromorphic systems of artificial intelligence and unconventional computing. These devices are known to produce a huge range of interesting phenomena through the interplay of regular, chaotic, and stochastic behavior. However, the character of these interplays as well as the instabilities responsible for different dynamical regimes are still poorly studied because of the difficulties in analyzing the complex stochastic dynamics of the memristive devices. In this paper, we introduce a new deterministic model justified from the Fokker–Planck description to capture the noise-driven dynamics that noise has been known to produce in the diffusive memristor. This allows us to apply bifurcation theory to reveal the instabilities and the description of the transition between the dynamical regimes.

© 2021 Author(s). All article content, except where otherwise noted, is licensed under a Creative Commons Attribution (CC BY) license (<http://creativecommons.org/licenses/by/4.0/>). <https://doi.org/10.1063/5.0056239>

Recently fabricated diffusive memristors¹ show a wide range of complex dynamics determined by the interplay of nanomechanical, heat, and electric degrees of freedom. If the diffusive memristor is connected to a simple circuit with a resistor in series and a capacitor in parallel, such a neuromorphic circuit demonstrates different types of oscillations, some of which are driven by dynamical features of the system and others are induced by noise. More interestingly, the system starts to demonstrate a new class of emerging phenomena, which can only appear due to the interplay of dynamical and noise-driven properties. To understand and control the system, we need to develop models that uncover such emerging mechanisms, this can be done by proper averaging over the stochastic dynamics and separating fast and slow degrees of freedom within the system, which is the goal of this paper.

I. INTRODUCTION

For the past decade, artificial intelligence and machine learning have witnessed a huge increase in their applications and their utilization in both academia and industry, with modern machine learning methods being applied in a huge range of fields, such as financial economics,² particle physics,^{3,4} and now even autonomous vehicles.^{5,6} However, with increasing applications and a constant

increase to the size of the data needed to run such models, we have begun to see the limits of modern computational architecture, such as an ever growing need for greater power consumption along with relying on unreasonably long time scales to complete such tasks. We have grown accustomed to constant improvements to computing power and the consistent miniaturization of computational components;⁷ to sustain this pattern, it is now clear that we need a new form of computing. Fortunately, a great area of promise is within that of neuromorphic computing, which attempts to replicate the information processing mechanisms found in biological circuits comprising neurons that enable rapid pattern recognition at an extraordinarily low power consumption. The first milestone in this direction is to produce an artificial memristor-based neuron, which has the same level of plasticity that biological neurons have or even to outperform them. These artificial neurons then allow for the development of hardware-based spiking neural network computing, which is close to impossible for current software implementation due to resource constraints.

In 1971, Chua⁸ published the seminal paper in which he postulated that there should be an additional, fourth fundamental circuit element. In observing that there was a form of symmetry between the interacting relationships of the four circuit variables, in particular, the current i , the charge q , the voltage v , and the flux linkage φ , there should be an additional circuit element linking flux

linkage and charge. This new element was named a “memristor.” In a future paper, Chua and Kang⁹ expanded on this original idea and introduced a new class of dynamical systems, which was called “memristive systems.” While the idea has been around since 1971, it was not until 2008 when HP labs¹⁰ had experimentally verified that the memristor did have a physical counterpart to its theoretical existence. The memristor is a two-terminal device, which has the unique property that its resistance is dependent on some internal variable, which can change when a current flowing through the memristor that is reminiscent to the dynamics of a biological neuron and synapse.

Since the experimental discovery of the memristor, there has been an emergence of different types of devices that fall under this category. For example, the so-called nonvolatile memristor¹¹ has the property of being able to maintain either the high- or low-resistive state after the external voltage has been removed.¹² The other recently developed volatile memristors switch back to the same resistive state (usually with high resistance) after a short relaxation time of the order of milliseconds after the external voltage has been removed (see, e.g., Ref. 1). The combination of volatile and non-volatile memristors allows for the realization of both artificial synapses and artificial neurons for more accurate mimicking of the behaviors observed in neural networks and, therefore, may be more suitable for the desired goal of neuromorphic computing (see, e.g., Ref. 13).

There have been many devices produced that would classify as a volatile memristor, of which they rely on different physical mechanisms for resistive switching.^{14–16} A new form of a volatile memristor has been fabricated and is called the diffusive memristor. This device produces resistive switching through the diffusion of Ag-metallic nanoclusters within SiO₂ from one terminal to another, and this forms a bridge between the two terminals.¹ The combination of mechanical, thermal, and electrical degrees of freedom allows this device to have a wide range of stochastic, dynamical, and sometimes chaotic behavior (see, e.g., Refs. 17 and 18). Not only is this memristor interesting from a mathematical viewpoint, the device can emulate both long-term and short-term plasticity,¹ meaning that it resembles biological cell mechanics closer than other memristive devices.

“Artificial neurons” based on different memristors have been produced,^{19–22} of which they are seemingly capable of showing regular spiking, which makes them an ideal candidate for oscillator-based computing,^{23,24} a new computational concept relying on accurate phase and frequency locking of synchronized oscillators. This, however, is problematic for the diffusive memristor as this device shows highly random spiking, but this may be advantageous when mimicking biological neurons where noise plays an essential role.²⁵

Even though the end goal for memristor research is to analyze large ensembles of interacting devices, it should be noted that each individual part of the memristive network should be investigated. Within this paper, we analyze a single artificial neuron based on the same diffusive memristor within,^{17,26} but instead of performing stochastic simulations, we formulate the corresponding Fokker–Planck equation for a diffusing Ag cluster and solve it by expanding the potential for the cluster up to the second order with respect to the particle deviation from its average trajectory. We then investigate the new system of ordinary differential equations to see

what deterministic mechanisms of spiking the system exhibits. We find that the deterministic model is capable of replicating the two main forms of spiking observed in the stochastic version, providing us with a better understanding of how to control the seemingly random spiking of stochastic diffusive artificial neurons.

II. MODELS AND METHODS

A. Memristor model

The memristor that has been investigated in this section will be a two-terminal device where Ag clusters (which we can also call particles) may travel from one terminal to another, and the distribution of these clusters will intern define the resistance of the memristor. A simple model that considers cluster diffusion coupled to the heat and electron dynamics^{1,13,26,27} can provide an accurate description of electric circuits with diffusive memristors. In a simplified version of that model for an artificial neuron circuit [see Fig. 1(a)], where only one Ag cluster is considered, it is still powerful enough to capture most experimental features and simultaneously allows one to quantitatively interpret the obtained results.¹⁷ The model is given as

$$\begin{cases} \eta \frac{dx}{dt} = -U(x) + qV + \sqrt{\eta T} \xi(t), \\ \frac{dT}{dt} = \frac{V^2}{\gamma R(x)} - \kappa(T - T_0), \\ \tau_c \frac{dV}{dt} = V_{ext} - \left(1 + \frac{R_{ext}}{R(x)}\right) V. \end{cases} \quad (1)$$

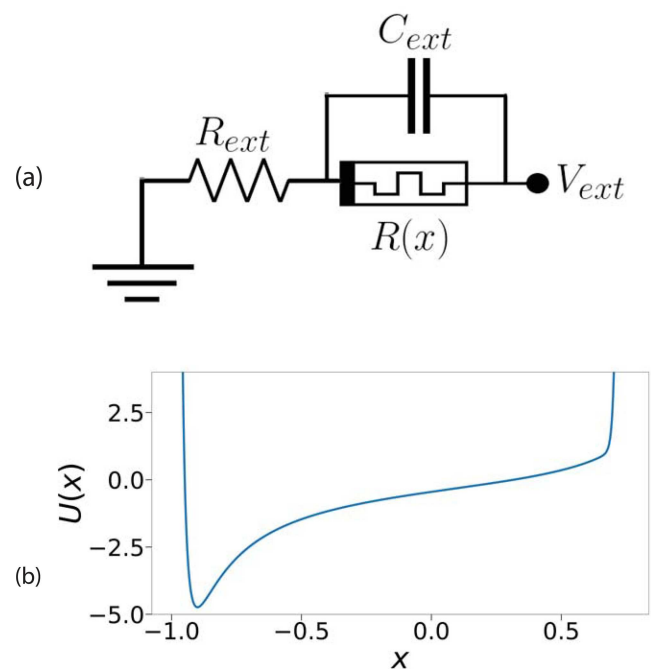


FIG. 1. (a) The circuit diagram of the model given by Eq. (1). (b) The memristor potential profile $U(x)$ given by Eq. (2).

Here, we have x defining the position of the particle, q is the electrical charge of the Ag cluster, V is the voltage between the two terminals, T is the temperature of the device, $\xi(t)$ is a zero-averaged δ -correlated Gaussian noise, and η is the effective viscosity of the Ag clusters in the SiO₂ matrix. The first of the three equations describes the motion of the particle in a tilted potential $U(x)$ under the influence of thermal noise and an externally applied electric field. We have used ' to denote the derivative with respect to x .

We model the potential as such,

$$\eta U(x) = \frac{0.05}{(x+1)^2} - \frac{1}{x+1} - \frac{0.5}{x-1} + (1.2x + 0.168)^{100}. \quad (2)$$

The contribution to this potential comes through (i) interfacial energy²⁶ favoring the cluster to be attracted to other non-movable clusters, forming filaments,^{28,29} or memristor terminals and (ii) interaction of the particle with inhomogeneities/pinning³⁰ and insulating matrix.³¹ The shape of $U(x)$ [Fig. 1(b)] was motivated by the experimental observation of hysteresis in current-voltage curves in both current- and voltage-driven regimes of volatile memristors,^{32–34} which means the co-existence of S- and N-types of negative differential resistance within the same current-voltage characteristic of a device (a similar property was found in superconductors³⁵). This is an important peculiarity of memristors, which makes them capable of generating different types of current pulses.³⁶

In order to reproduce that hysteretic behavior, the combination of the above-mentioned forces should result in a potential with a negative second order derivative inside a region between the memristor terminals to prohibit an adiabatic motion of the cluster when driven by the constant voltage; the potential we consider here has such a region of a negative second derivative. We found it appropriate to use the classical model of the central field force potential,³⁷ which forms an attracting well next to the left memristor terminal (close to $x = -1$), while the particle cannot reach the right terminal due to a strong repulsive pinning [modeled by the last term of Eq. (2)] discussed in Ref. 30.

The second equation in the system (1) models the heat exchange³⁸ within the device with the Joule heat source, which is controlled by the memristors resistance $R(x)$ and heat capacitance γ , and the heat sink is determined by the heat-transfer coefficient κ and the bath temperature T_0 .

The third equation is Kirchhoff's rule for the circuit under consideration [Fig. 1(a)], where we define external resistance with R_{ext} , external voltage with V_{ext} , and so-called RC-time, τ_c , of the capacitor charging.

The resistance of the memristor is dependent on the current position of the particle. We assume that given the particle fluctuates between the two electrodes and that the electrons tunnel from one terminal to the other through the particle (somewhat similar to electron shuttling, see, e.g., Ref. 39), this results in a fluctuating resistance. The tunneling resistance between one of the electrodes and the particle and the second electrode and the particle are, respectively, $R_1 \propto \exp[(1-x)/\lambda]$ and $R_2 \propto \exp[(1+x)/\lambda]$, where we define λ (see, e.g., Ref. 40) to equal the tunneling length, which implies that all resistances are normalized by the lowest resistance of the memristor. This allows us to rewrite the total resistance as $R(x) = R_1 + R_2 = R_0 \cosh(x/\lambda)$; below, we will normalize all resistances to $R_0 = 1$; that is, R_0 is our unit for resistance. Note that the

current through the memristor can be calculated using Ohm's law, $I = V/R(x)$. The circuit shown in Fig. 1(a) is called an "artificial neuron"²² within the literature because it has the capability to produce short impulses, which can be viewed in a similar manner as the spiking that is observed in biological cells.

B. Deterministic model

In a series of works performed by the research group of V. S. Anishchenko and their collaborators, it was demonstrated that certain stochastic phenomena can be observed in purely deterministic chaotic systems,^{41,42} while the effects typical for the deterministic oscillators can also occur in systems with noise-induced dynamics.^{43–45} Partly, such universality of the phenomena can be explained by the fact that often noisy dynamics and deterministic chaos in dynamical systems demonstrate similar statistical properties.^{46,47} On the other hand, noise can induce a distinct time scale in the system, which makes the dynamics quite coherent. Moreover, under certain conditions, small random fluctuations are able to evoke the dynamics demonstrating the properties of deterministic chaos.⁴⁸ All these findings suggest that under certain assumptions, the interplay between stochastic and deterministic phenomena allows for a deterministic description, which could simplify the analysis.

In our case, we start with by considering the Fokker-Planck equation corresponding to the model (1), which is a partial differential equation in the 4D (t, x, V, T) space. For simplicity, we consider the situation when temperature and voltage change slowly compared to particle diffusion. In this case, we can state that both temperature and voltage can be described by ordinary differential equations with an average conductance $(1/R(x))$ determined by a reduced Fokker-Planck equation for the particle diffusion in the (t, x) space, namely,

$$\begin{cases} \frac{dT}{dt} = \frac{V^2}{\gamma} \left\langle \frac{1}{R(x)} \right\rangle - \kappa(T - T_0), \\ \frac{dV}{dt} = \frac{1}{\tau_c} \left[V_{ext} - \left(1 + R_{ext} \left\langle \frac{1}{R(x)} \right\rangle \right) V \right], \\ \eta \frac{\partial P}{\partial t} = - \frac{\partial}{\partial x} [-U'(x) + qV] P + T \frac{\partial^2 P}{\partial x^2}. \end{cases} \quad (3)$$

We have used the angled brackets to represent the averaged value. If we now approximate the derivative of the potential as $U'(x) = U'(x_0) + U''(x_0)(x - x_0)$, then we shall seek a solution of the Fokker-Planck equation in the form $P = A \frac{1}{\sqrt{\Delta}} e^{-\frac{(x-x_0)^2}{\Delta}}$, with two new variables $x_0(t)$ and $\Delta(t)$, which describes the particle's average position and the standard deviation of thermal fluctuations of the particle's motion. This then lets us have four ordinary differential equations,

$$\begin{cases} \eta \frac{dx_0}{dt} = -U'(x_0) + qV, \\ \eta \frac{d\Delta}{dt} = 4T - 2\Delta U''(x_0), \\ \frac{dT}{dt} = \frac{V^2}{\gamma} \left\langle \frac{1}{R(x)} \right\rangle - \kappa(T - T_0), \\ \frac{dV}{dt} = \frac{1}{\tau_c} \left[V_{ext} - \left(1 + R_{ext} \left\langle \frac{1}{R(x)} \right\rangle \right) V \right], \end{cases} \quad (4)$$

where

$$\left\langle \frac{1}{R(x)} \right\rangle = \frac{A}{\sqrt{\Delta}} \int_{-\infty}^{\infty} \frac{1}{\cosh(\frac{x}{\lambda})} e^{-\frac{(x-x_0)^2}{\Delta}} dx. \quad (5)$$

To estimate this integral, we approximate $1/\cosh(x/\lambda)$ for the particle located between memristor electrodes $-1 < x < 1$ (with $x = \pm 1$ corresponding to the left/right electrode and x normalized by half of the distance between electrodes) by a sum,

$$\frac{1}{\cosh(\frac{x}{\lambda})} \approx \sum P_i e^{-b_i x^2}. \quad (6)$$

By using the least squares regression for four terms in the sum (6) and $\lambda = 0.12$, we estimate the parameters P_i and b_i as $P_1 = 0.1398$, $P_2 = 0.4306$, $P_3 = 0.3509$, $P_4 = 0.0785$; $b_1 = 95.3853$, $b_2 = 36.8889$, $b_3 = 14.0560$, $b_4 = 5.3923$. Now, evaluating the integral (5) leads to

$$\left\langle \frac{1}{R(x)} \right\rangle = \sum P_i e^{-\frac{b_i x_0^2}{1+b_i \Delta}} \frac{1}{\sqrt{1+b_i \Delta}}. \quad (7)$$

Substituting (7) into (4) allows us to derive the set of equations that we will study in this paper to model the artificial neuron

$$\begin{cases} \frac{dx_0}{dt} = M(-U'(x_0) + qV), \\ \frac{d\Delta}{dt} = M(4T - 2\Delta U''(x_0)), \\ \frac{dT}{dt} = \frac{V^2}{\gamma} \sum P_i e^{-\frac{b_i x_0^2}{1+b_i \Delta}} \frac{1}{\sqrt{1+b_i \Delta}} - \kappa(T - T_0), \\ \tau_c \frac{dV}{dt} = V_{ext} - \left(1 + R_{ext} \sum P_i e^{-\frac{b_i x_0^2}{1+b_i \Delta}} \frac{1}{\sqrt{1+b_i \Delta}} \right) V, \end{cases} \quad (8)$$

with $M = 1/\eta$.

Below, numerical simulations of the system (8) are carried out by use of the *LSODA* package⁴⁹ with step size $t = 0.0001$. The numerical simulations for the oscillations are run with the same values used for the bifurcation analysis: $Mq = 0.50$, $\tau_c = 2$, $R_{ext} = 300$, $M = 0.3$, $\gamma = 16.7$, $\kappa = 0.9$, and $T_0 = 0$. For numerical simulations relating to the figures, Figs. 3 and 4, we fix voltage to $V_{ext} = 186.8$.

III. SPIKING REGIMES

Within the artificial neuron model [Eq. (1)], there are two different spiking regimes,¹⁷ one associated with charge/discharge cycles and the other being produced due to a much slower heating-cooling cycle caused by thermal effects. The former spiking phenomena can be explained as such: when the external voltage supply V_{ext} is originally switched on, the memristor is at a high resistive state and the capacitor begins to charge due to the current flowing through it. However, at a certain voltage, V , it is great enough to force the particle to escape the potential well and starts to approach the center point of the device, and therefore, the resistance, $R(x)$, enters its lowest value. This then causes the capacitor to discharge, leading to a decrease in the voltage, the resistance then begins to increase once more and the particle re-enters the well and this results in the capacitor to start recharging, resembling the Pearson–Anson effect.⁵⁰

The second spiking regime can only be achieved via the interplay of stochastic and deterministic dynamics in the original model (1) and is associated with the particle being moved due to thermal effects within the device, going through heating and cooling cycles. Previous works have shown that this regime involves noise-induced phenomena;¹⁷ however, the dynamical mechanisms and related instabilities capable to evoke such spiking behavior still remain unclear. To investigate these open questions, we utilize the model (8).

IV. BIFURCATION ANALYSIS AND NUMERICAL RESULTS

The analysis of the mechanisms governing the emergence of the spiking phenomena in the model (8), which describes the circuit in Fig. 1(a), is summarized in the bifurcation diagram presented in Fig. 2. Here, the y axis is representing the maximum and minimum values of the position, x_0 , and the horizontal axis is representing the external voltage, V_{ext} .

The bifurcation diagram in Fig. 2 reveals three branches of the fixed points (red and black points), which give rise to the stable solutions. They correspond to the positions, x_0 close to -0.9 (lower branch), 0 (middle branch), and 0.6 (upper branch). The coexistence of these branches for the same values of V_{ext} can explain the hysteretic transitions in the current–voltage characteristics and the multistability measured previously in diffusive memristors (see, e.g., Ref. 27).

For low voltages V_{ext} , the system demonstrates the only stable solution, which is a lower branch equilibrium (red point) at x_0 close to -0.9 corresponding to the potential minimum of $U(x)$; see Fig. 1(b). The fixed point remains stable until an Andronov–Hopf bifurcation at $V_{ext} \approx 49.1$, where it loses its stability, and then remains unstable for larger V_{ext} (black points). The Andronov–Hopf bifurcation gives birth to a stable periodic orbit, whose extreme values of x are shown by green points. These small-amplitude stable oscillations rapidly disappear due to a saddle-node bifurcation at $V_{ext} \approx 51.9$, which implies a collision of a stable cycle (green points) with an unstable limit cycle (pink points). Another saddle-node bifurcation for limit cycles leads to the reappearance of stable self-oscillations at $V_{ext} \approx 51.1$. These periodic oscillations correspond to the first type of spiking generated by charge–discharge cycles in the circuit. As V_{ext} further increases, this spiking regime ceases out as the result of the saddle-node bifurcation at $V_{ext} \approx 239.9$. Thus, the mechanisms for the onset of the first type of spiking are associated with Andronov–Hopf and saddle-node bifurcations for the limit cycles. These mechanisms are consistent with the generation of charge–discharge spiking in other types of memristive circuits, e.g., based on NbO_x memristors previously analyzed in Ref. 22.

The middle branch demonstrates an Andronov–Hopf bifurcation at $V_{ext} \approx 203.6$, which for decreasing/increasing V_{ext} corresponds to the appearance/disappearance of stable periodic solutions. With a decrease of V_{ext} , this limit cycle disappears through the saddle-node bifurcation at $V_{ext} \approx 186.7$. For $V_{ext} > 203.6$, the fixed point of this branch remains stable until $V_{ext} \approx 280.4$, where it becomes unstable through another Andronov–Hopf bifurcation, which originates an unstable periodic solution (pink dots). This

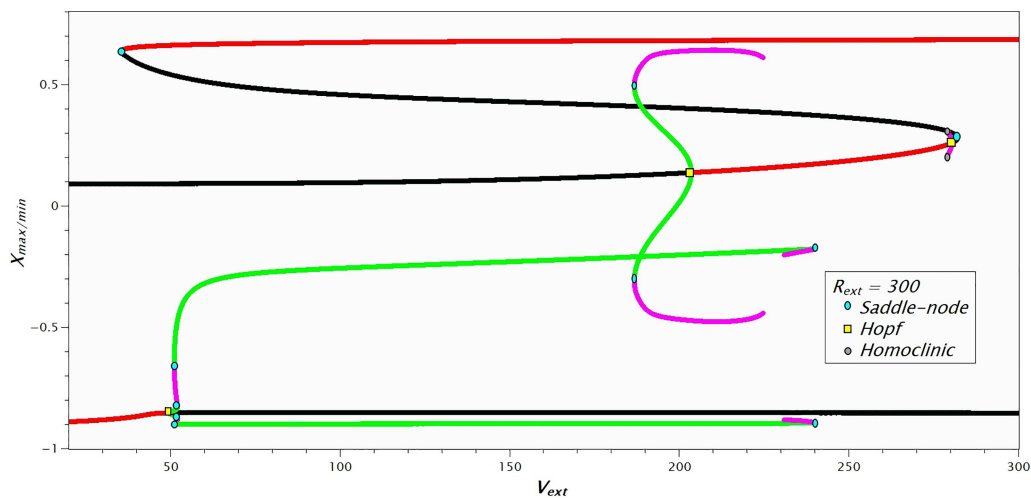


FIG. 2. One-dimensional bifurcation diagram (at $R_{ext} = 300$). The red color indicates the stable fixed point, the black is for an unstable one, and green and pink are for maximum and minimum values of x_0 on stable and unstable limit cycles, respectively.

unstable orbit eventually touches the unstable fixed point, manifesting a homoclinic bifurcation,^{51–53} and as such, the orbit disappears. This branch of fixed points stops its existence at $V_{ext} \approx 282.1$, where it collides with a branch of unstable fixed points implying a saddle-node bifurcation. The latter branch of unstable fixed points involves in another saddle-node bifurcation at $V_{ext} \approx 35.3$, which induces an upper branch of a stable fixed point. For $V_{ext} > 35.3$, these equilibria are stable and represent a high-resistance regime to which the system switches when the V_{ext} is gradually increased.

Note that the unstable limit cycles shown in the diagram by pink color points are induced either through the saddle-node bifurcation or through global instabilities including that shown by the gray circle homoclinic bifurcation, which manifest themselves in an abrupt appearance and disappearance of finite-amplitude periodic solutions.

Figure 3 compares the stable self-oscillations (green points in Fig. 2) corresponding to the lower and middle branches for the same value of $V_{ext} = 186.8$. The corresponding projections of phase trajectories are shown in (a). The blue curve, corresponding to the lower branch, demonstrates large oscillations of the voltage across the memristor V , which reflects the charge–discharge cycles defined by the capacitance in the circuit [see Fig. 1(a)]. This limit cycle corresponds to fast uniform oscillations of $I(t)$ as illustrated in (b). The stable limit cycle born in the middle branch is shown in (a) by the red curve, while the corresponding current oscillations are illustrated in (c). In contrast to the previous case, these oscillations do not involve the large variation of V , and their periodicity is rather defined by a “cooling–heating” cycle. Since the temperature changes are quite inertial, these oscillations are slower than charge–discharge oscillations [compare (b) and (c)]. Thus, the middle branch produces the stable self-oscillations representing the second type of spiking.

Remarkably, previously, it has been shown that “cooling–heating” type of spiking is essentially a noise-induced

phenomenon.¹⁷ However, our approach allowed us to grasp it using a purely deterministic model. This suggests an interpretation of the mechanisms for the onset of such spiking in terms of bifurcation theory. In particular, our results suggest that the mechanisms for the appearance of the second type of spiking in diffusive memristors can be interpreted as saddle-node and Andronov–Hopf bifurcations for noise-induced cycles.

Our further study showed that the revealed bifurcation mechanisms of the first and second type of spiking are robust against the variation of the memristor parameters. However, in certain ranges, new complex dynamical regimes can appear in the system, including ones that resemble chaotic oscillations. An example of such dynamics is shown in Fig. 4, which was calculated for $M = 0.003$ and $V_{ext} = 186.8$. The current oscillations in such a regime illustrated in (a) demonstrate spiking behavior with quite random variations of the spike heights and rather erratic fast background oscillations near $I \approx 0.2$. The chaotic character of such dynamics becomes even more evident in the projection of the corresponding phase trajectory depicted in (b). Here, the current spikes correspond to long irregular excursions in the phase space, while the background oscillations are represented by fast chaotic rotations in the vicinity of $x_0 \approx -0.65$. The large fluctuations of V suggest that this regime involves a charge–discharge mechanism.

The detailed analysis of such dynamics is beyond the scope of this paper and will be a subject of further investigation. Remarkably though, some types of the memristive devices have been known to show chaotic phenomena; see, e.g., Ref. 54. However, the diffusive memristors are essentially stochastic devices, in which the deterministic chaos, if it exists, is practically impossible to register because of the presence of a non-negligible noise. Our results suggest that under certain conditions, this device can demonstrate chaos-like dynamics in the statistical description, similarly to the phenomena previously reported for an ensemble of noisy oscillators.⁵⁵

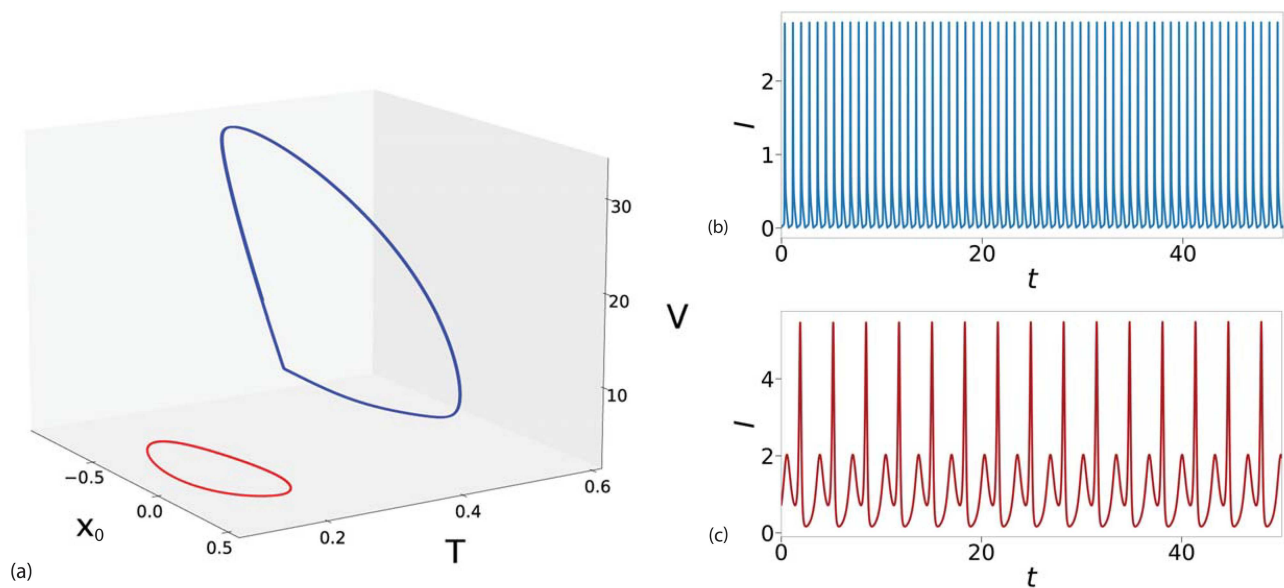


FIG. 3. (a) Phase space of x_0 , T , and V corresponding to the coexistence of two limit cycles at $V_{ext} = 186.8$. The blue line corresponding to the first form of spiking and the red line corresponding to the second spiking mode. (b) Time realization $I(t)$ corresponding to the self-sustained periodic oscillations due to charge–discharge effects. (c) Time realization $I(t)$ corresponding to the self-sustained periodic oscillations due to heating–cooling effects.

V. CONCLUSION

In this paper, we present an approach to model stochastic phenomena in circuits involving diffusive memristors in a deterministic model. The electric properties of these devices are determined by Ag clusters drifting between the terminals under the action of an electric field, heat exchange with the device, and thermal fluctuations.^{1,13,26,27} Specifically, we propose a model of the diffusive memristor where the Langevin equation describing the motion of an Ag-metallic

nanocluster is replaced by its Fokker–Planck counterpart. Approximating a solution of the Fokker–Planck equation by a Gaussian distribution allows us to obtain a set of deterministic equations for the average particle position and the width of the distribution related to cluster fluctuations. Our analysis of the obtained set of ordinary differential equations shows that the model allows for describing two different spiking regimes, which were originally obtained in the full stochastic simulation¹⁷ of the original set of stochastic equation (1).

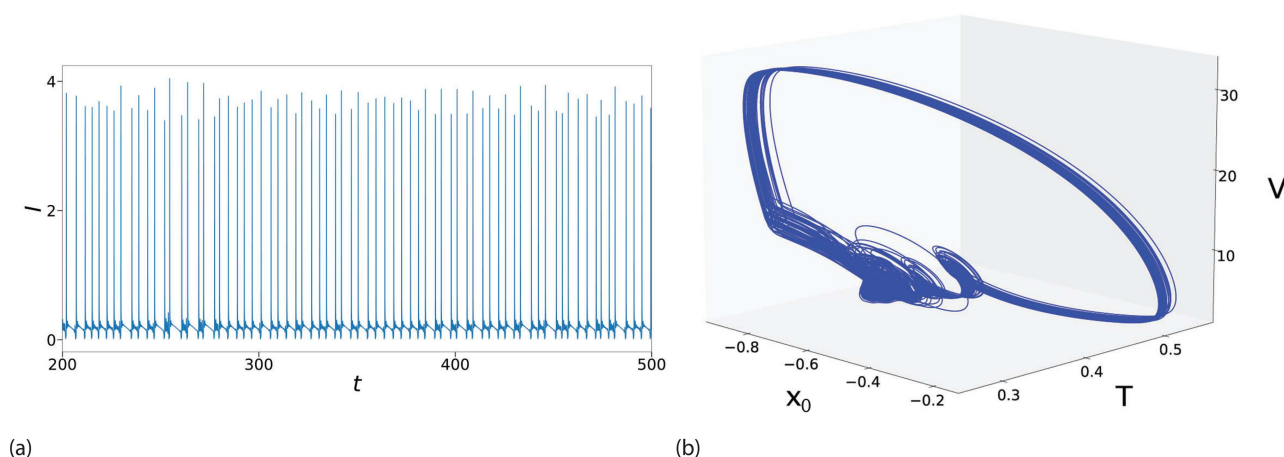


FIG. 4. Chaotic time realization of $I(t)$ (a) and the corresponding projection of the phase trajectory (b) at $M = 0.003$.

We investigated this new system and showed that the predominant mechanisms that lead to the onset of different spiking regimes are associated with Andronov–Hopf bifurcations and saddle-node bifurcations for limit cycles. We also demonstrated that for certain parameters, the new model can demonstrate chaos-like dynamics. The possibility to describe the mechanisms of stochastic spiking in diffusive memristors in terms of bifurcation and chaos theories paves a new avenue for informing the design of memristive circuits and controlling their dynamical regimes. The latter is crucially important for the development of memristive systems for artificial intelligence and neuromorphic computers.

ACKNOWLEDGMENTS

This work was supported by the Engineering and Physical Sciences Research Council (EPSRC) (Grant No. EP/S032843/1).

DATA AVAILABILITY

The data that support the findings of this study are available from the corresponding author upon reasonable request.

REFERENCES

- Z. Wang, S. Joshi, S. E. Savel'ev, H. Jiang, R. Midya, P. Lin, M. Hu, N. Ge, J. P. Strachan, Z. Li *et al.*, “Memristors with diffusive dynamics as synaptic emulators for neuromorphic computing,” *Nat. Mater.* **16**, 101 (2017).
- M.-W. Hsu, S. Lessmann, M.-C. Sung, T. Ma, and J. E. Johnson, “Bridging the divide in financial market forecasting: Machine learners vs financial economists,” *Expert Syst. Appl.* **61**, 215–234 (2016).
- A. Radovic, M. Williams, D. Rousseau, M. Kagan, D. Bonacorsi, A. Himmel, A. Aurisano, K. Terao, and T. Wongjirad, “Machine learning at the energy and intensity frontiers of particle physics,” *Nature* **560**, 41 (2018).
- G. Carleo, I. Cirac, K. Cranmer, L. Daudet, M. Schuld, N. Tishby, L. Vogt-Maranto, and L. Zdeborová, “Machine learning and the physical sciences,” *Rev. Mod. Phys.* **91**, 045002 (2019).
- Y. Ma, Z. Wang, H. Yang, and L. Yang, “Artificial intelligence applications in the development of autonomous vehicles: A survey,” *IEEE/CAA J. Autom. Sin.* **7**, 315–329 (2020).
- I. Yaqoob, L. U. Khan, S. M. A. Kazmi, M. Imran, N. Guizani, and C. S. Hong, “Autonomous driving cars in smart cities: Recent advances, requirements, and challenges,” *IEEE Netw.* **34**, 174–181 (2020).
- R. Schaller, “Moore’s law: Past, present and future,” *IEEE Spectr.* **34**, 52–59 (1997).
- L. Chua, “Memristor—The missing circuit element,” *IEEE Trans. Circuit Theory CT-18*, 507 (1971).
- L. Chua and S. Kang, “Memristive devices and systems,” *Proc. IEEE* **64**, 209 (1976).
- D. B. Strukov, G. S. Snider, D. R. Stewart, and R. S. Williams, “The missing memristor found,” *Nature* **453**, 80–83 (2008).
- G. Huang and Y. Ho, in *Advances in Non-Volatile Memory and Storage Technology*, edited by Y. Nishi (Woodhead Publishing, 2014), pp. 370–397.
- R. Wang, J.-Q. Yang, J.-Y. Mao, Z.-P. Wang, S. Wu, M. Zhou, T. Chen, Y. Zhou, and S.-T. Han, “Recent advances of volatile memristors: Devices, mechanisms, and applications,” *Adv. Intell. Syst.* **2**, 2000055 (2020).
- Z. Wang, S. Joshi, S. Savel'ev, W. Song, R. Midya, Y. Li, M. Rao, P. Yan, S. Asapu, Y. Zhuo, H. Jiang, P. Lin, C. Li, J. H. Yoon, N. K. Upadhyay, J. Zhang, M. Hu, J. P. Strachan, M. Barnell, Q. Wu, H. Wu, R. S. Williams, Q. Xia, and J. J. Yang, “Fully memristive neural networks for pattern classification with unsupervised learning,” *Nat. Electron.* **1**, 137–145 (2018).
- Q. Hua, H. Wu, B. Gao, M. Zhao, Y. Li, X. Li, X. Hou, M.-F. (Marvin) Chang, P. Zhou, and H. Qian, “A threshold switching selector based on highly ordered Ag nanodots for X-point memory applications,” *Adv. Sci.* **6**, 1900024 (2019).
- S. Saitoh and K. Kinoshita, “Oxide-based selector with trap-filling-controlled threshold switching,” *Appl. Phys. Lett.* **116**, 112101 (2020).
- W. Yi, K. K. Tsang, S. K. Lam, X. Bai, J. A. Crowell, and E. A. Flores, “Biological plausibility and stochasticity in scalable VO₂ active memristor neurons,” *Nat. Commun.* **9**, 4661 (2018).
- Y. Ushakov, A. Balanov, and S. Savel'ev, “Role of noise in spiking dynamics of diffusive memristor driven by heating-cooling cycles,” *Chaos, Solitons Fractals* **145**, 110803 (2021).
- A. Wojtusik, A. Balanov, and S. Savel'ev, “Intermittent and metastable chaos in a memristive artificial neuron with inertia,” *Chaos, Solitons Fractals* **142**, 110383 (2021).
- X. Zhang, Y. Zhuo, Q. Luo, Z. Wu, R. Midya, Z. Wang, W. Song, R. Wang, N. K. Upadhyay, Y. Fang, F. Kiani, M. Rao, Y. Yang, Q. Xia, Q. Liu, M. Liu, and J. J. Yang, “An artificial spiking afferent nerve based on Mott memristors for neurorobotics,” *Nat. Commun.* **11**, 51 (2020).
- S. Kumar, R. Williams, and Z. Wang, “Third-order nanocircuit elements for neuromorphic engineering,” *Nature* **585**, 518 (2020).
- X. Zhang and K. Long, “Improved learning experience memristor model and application as neural network synapse,” *IEEE Access* **7**, 15262–15271 (2019).
- B. Johnson, K. Brahim, A. Balanov, S. Savel'ev, and P. Borisov, “Transition from noise-induced to self-sustained current spiking generated by a NbO_x thin film threshold switch,” *Appl. Phys. Lett.* **118**, 023502 (2021).
- D. Vodenicarevic, N. Locatelli, F. A. Araujo, J. Grollier, and D. Querlioz, “A nanotechnology-ready computing scheme based on a weakly coupled oscillator network,” *Sci. Rep.* **7**, 44772 (2017).
- G. Csaba and W. Porod, “Coupled oscillators for computing: A review and perspective,” *Appl. Phys. Rev.* **7**, 011302 (2020).
- M. L. Simpson, C. D. Cox, M. S. Allen, J. M. McCollum, R. D. Dar, D. K. Karig, and J. F. Cooke, “Noise in biological circuits,” *Wiley Interdiscip. Rev. Nanomed. Nanobiotechnol.* **1**, 214–225 (2009).
- H. Jiang, D. Belkin, S. E. Savel'ev, S. Lin, Z. Wang, Y. Li, S. Joshi, R. Midya, C. Li, M. Rao, M. Barnell, Q. Wu, J. J. Yang, and Q. Xia, “A novel true random number generator based on a stochastic diffusive memristor,” *Nat. Commun.* **8**, 882 (2017).
- R. Midya, Z. Wang, J. Zhang, S. E. Savel'ev, C. Li, M. Rao, M. H. Jang, S. Joshi, H. Jiang, P. Lin, K. Norris, N. Ge, Q. Wu, Z. Barnell, M. amd Li, H. L. Xin, R. S. Williams, Q. Xia, and J. J. Yang, “Anatomy of Ag/Hafnia-based selectors with 1010 nonlinearity,” *Adv. Mater.* **29**, 1604457 (2017).
- S. E. Savel'ev, A. S. Alexandrov, A. M. Bratkovsky, and R. S. Williams, “Molecular dynamics simulations of oxide memory resistors (memristors),” *Nanotechnology* **22**, 254011 (2011).
- S. E. Savel'ev, A. S. Alexandrov, A. M. Bratkovsky, and R. S. Williams, “Molecular dynamics simulations of oxide memristors: Thermal effects,” *Appl. Phys. A* **102**, 891 (2011).
- W. Yi, S. Savel'ev, G. Medeiros-Ribeiro, F. Miao, M.-X. Zhang, J. Yang, A. Bratkovsky, and R. Williams, “Quantized conductance coincides with state instability and excess noise in tantalum oxide memristors,” *Nat. Commun.* **7**, 11142 (2016).
- S. E. Savel'ev, A. S. Alexandrov, A. M. Bratkovsky, and R. S. Williams, “Molecular dynamics simulations of oxide memristors: Crystal field effects,” *Appl. Phys. Lett.* **99**, 053108 (2011).
- S. Kumar, R. S. Williams, and Z. Wang, “Third-order nanocircuit elements for neuromorphic engineering,” *Nature* **585**, 518–523 (2020).
- S. Kumar, J. P. Strachan, and R. S. Williams, “Chaotic dynamics in nanoscale NbO₂ Mott memristors for analogue computing,” *Nature* **548**, 318–321 (2017).
- I. Messaris, R. Tetzlaff, A. Ascoli, R. Williams, S. Kumar, and L. Chua, “A simplified model for a NbO₂ Mott memristor physical realization,” in *2020 IEEE International Symposium on Circuits and Systems (ISCAS)* (IEEE, 2020), pp. 1–5.
- V. R. Misko, S. Savel'ev, A. L. Rakhmanov, and F. Nori, “Negative differential resistivity in superconductors with periodic arrays of pinning sites,” *Phys. Rev. B* **75**, 024509 (2007).
- Y. Ushakov, A. Akther, P. Borisov, D. Pattnaik, S. Savel'ev, and A. Balanov, “Deterministic mechanisms of spiking in diffusive memristors,” *Chaos, Solitons Fractals* **149**, 110997 (2021).
- H. Goldstein, C. Poole, and J. Safko, *Classical Mechanics*, 3rd ed. (Pearson, 2001).

- ³⁸A. S. Alexandrov, A. M. Bratkovsky, B. Bridle, S. E. Savel'ev, D. B. Strukov, and R. S. Williams, "Current-controlled negative differential resistance due to Joule heating in TiO₂," *Appl. Phys. Lett.* **99**, 202104 (2011).
- ³⁹A. V. Moskalenko, S. N. Gordeev, O. F. Koentjoro, P. R. Raithby, R. W. French, F. Marken, and S. E. Savel'ev, "Nanomechanical electron shuttle consisting of a gold nanoparticle embedded within the gap between two gold electrodes," *Phys. Rev. B* **79**, 241403 (2009).
- ⁴⁰S. E. Savel'ev, F. Marchesoni, and A. M. Bratkovsky, "Mesoscopic resistive switch: Non-volatility, hysteresis and negative differential resistance," *Eur. Phys. J. B* **86**, 501 (2013).
- ⁴¹V. S. Anishchenko, A. B. Neiman, and M. A. Safanova, "Stochastic resonance in chaotic systems," *J. Stat. Phys.* **70**, 183–196 (1993).
- ⁴²V. S. Anishchenko, A. B. Neiman, A. N. Silchenko, and I. A. Khovanov, "Phase synchronization of switchings in stochastic and chaotic bistable systems," *Dyn. Stab. Syst.* **14**, 211–231 (1999).
- ⁴³V. Anishchenko, V. Astakhov, A. Neiman, T. Vadivasova, and L. Schimansky-Geier, *Nonlinear Dynamics of Chaotic and Stochastic Systems: Tutorial and Modern Developments*, Springer Series in Synergetics (Springer, Berlin, 2007).
- ⁴⁴S. Astakhov, A. Feoktistov, V. S. Anishchenko, and J. Kurths, "Synchronization of multi-frequency noise-induced oscillations," *Chaos* **21**, 047513 (2011).
- ⁴⁵N. Semenova, A. Zakharova, V. Anishchenko, and E. Schöll, "Coherence-resonance chimeras in a network of excitable elements," *Phys. Rev. Lett.* **117**, 014102 (2016).
- ⁴⁶V. S. Anishchenko, T. E. Vadivasova, J. Kurths, G. A. Okrokvertskhov, and G. I. Strelkova, "Autocorrelation function and spectral linewidth of spiral chaos in a physical experiment," *Phys. Rev. E* **69**, 036215 (2004).
- ⁴⁷V. S. Anishchenko, T. E. Vadivasova, G. A. Okrokvertskhov, and G. I. Strelkova, "Statistical properties of dynamical chaos," *Phys.-Usp.* **48**, 151–166 (2005).
- ⁴⁸V. S. Anishchenko and H. Herzel, "Noise-induced chaos in a system with homoclinic points," *Z. Angew. Math. Mech.* **68**, 317–318 (1988).
- ⁴⁹L. Petzold, "Automatic selection of methods for solving stiff and nonstiff systems of ordinary differential equations," *SIAM J. Sci. Stat. Comput.* **4**, 136–148 (1983).
- ⁵⁰S. Pearson and H. Anson, "Demonstration of some electrical properties of neon-filled lamps," *Proc. Phys. Soc. London* **34**, 175 (1921).
- ⁵¹J. Guckenheimer and P. J. Holmes, *Nonlinear Oscillations, Dynamical Systems, and Bifurcations of Vector Fields* (Springer-Verlag, New York, 1983).
- ⁵²V. S. Anishchenko, *Dynamical Chaos—Models and Experiments. Appearance Routes and Structure of Chaos in Simple Dynamical Systems* (World Scientific Publishing, Singapore, 1995).
- ⁵³Y. Kuznetsov, *Elements of Applied Bifurcation Theory* (Springer-Verlag, New York, 2004).
- ⁵⁴S. Kumar, J. Strachan, and R. Williams, "Chaotic dynamics in nanoscale NbO₂ Mott memristors for analogue computing," *Nature* **548**, 318–321 (2017).
- ⁵⁵M. A. Zaks, A. B. Neiman, S. Feistel, and L. Schimansky-Geier, "Noise-controlled oscillations and their bifurcations in coupled phase oscillators," *Phys. Rev. E* **68**, 066206 (2003).